10th International Conference on Composite Science and Technology
ICCST/10
A.L. Araúo, J.R. Correia, C.M. Mota Soares, et al. (Editors)

INFLUENCE OF THE ELASTOMER LAYER POSITION ON THE LOW-VELOCITY IMPACT BEHAVIOR OF COMPOSITE/STEEL/ELASTOMER LAMINATES

Denise Düring*, Daniel Stefaniak*, Christian Hühne*

*DLR - German Aerospace Center - Institute of Composite Structures and Adaptive Systems
Lilienthalplatz 7, 38108 Braunschweig, Germany
denise.duering@dlr.de

Keywords: Hybrid Composite, FML, Laminate, Low-velocity Impact, Impact Behaviour.

Summary: *The influence of the elastomer layer position in a composite/steel/elastomer hybrid-material structure on the low-velocity impact behaviour is investigated in the presented study. Three different layer positions were investigated regarding their influence on the indentation depth and delaminations as well as the impact force evolution. It could be found that the positioning of the elastomer layer in the center plane of the CFRP support structure minimizes the destruction of internal and external damage because of a reduction of the stiffness. When the elastomer layer is located near the impacted surface, the surface damage through indentation is the predominant damage type caused by plastic deformation of the covering steel layer.*

1. INTRODUCTION

In aeronautical applications Carbon-Fibre Reinforced Plastics (CFRPs) have been established due to their advantageous stiffness- and strength-to-weight ratio. However, it appears that further development is limited by the material properties of conventional FRPs. That raises the demand for new material combinations to benefit from the favourable material properties of the different components. For example, Fiber Metal Laminates (FMLs) containing aluminum or steel show an increased impact resistance and residual strength after impact in comparison to CFRP structures [1–3]. Aerospace structures are often subject to impact by sand, rain, hail, and larger objects [4–6]. One problem is the weak erosion resistance of conventional CFRPs [7]. The impact of larger objects such as maintenance tools or hail can seriously damage the CFRP structure. Especially low-velocity impacts with high impact masses and velocities up to 10 m/s often result in serious intra- and interlaminar failure without being detectable [8, 9]. This requires a certain damage tolerance of the structure. Since CFRP structures do not meet those requirements, a new material combination has to be established. For erosion protection, the application of a steel layer on the erosion-prone surfaces is suitable because the erosion resistance of stainless steel is at least one order of magnitude higher compared to CFRP [10]. Sarlin et al. showed that the addition of a rubber layer to a GFRP structure can absorb the impact energy partially and decreases the internal damage for high velocity impacts [11]. The aim of the presented work is to identify a beneficial combination of several materials to obtain an increased

impact resistance and to avoid severe structural damage at usual impact events like hail strike. The basic CFRP structure is covered by one single steel foil layer for erosion resistance. A CFRP layer surrounded by two GFRP layers on top and bottom serves as a resistance heating for de-icing.

In previous studies the influence of different steel foil thicknesses and the addition of an elastomer layer to a CFRP/GFRP/steel hybrid structure on the low velocity impact response has already been investigated [12]. In the present work the position of the elastomer layer was varied and three different laminate configurations were examined. The elastomer layer was applied between the resistance heating and the CFRP structure, in the center layer of the CFRP structure and in the lower third of the CFRP structure. The influence of the elastomer position on internal and external damage was analyzed.

2. EXPERIMENT

2.1 Materials

Three different hybrid material configurations were tested. All of them contained a basic structure consisting of an 18-ply quasi-isotropic layup: $[\pm 45/0/\pm 45/90/\pm 45/(0)_2/\pm 45/90]_S$ with a nominal thickness of 5.13 mm. Additionally, one woven CFRP layer surrounded by two GFRP-layers on top and bottom built the resistance heating and was applied on the basic structure. Both GFRP and CFRP are preimpregnated fibers with an MTM44-1 resin (Cytec). The erosion protection layer, an X10CrNi18-8 stainless steel with a thickness of 0.125 mm, was roughened and treated in a sol-gel process introduced by Stefaniak et al. [3]. The 0.5 mm elastomer layer (an Ethylene Propylene Diene Monomer = EPDM) was applied on three different positions in each tested configuration. Firstly the elastomer layer was positioned between the heating and the CFRP basic structure (Layer 7), secondly in the middle plane of the CFRP main structure (Layer 16) and thirdly in the lower third of the CFRP structure (Layer 20). Consequently, the short designations for the sample configurations are L7, L16 and L20. Figure 1 shows the schematic layup of the basic structure and the three elastomer layer positions. The specimens with a nominal overall thickness of 6.48 mm were laid up by hand and finally cured according to manufacturer recommendations [13]. The details of the constituents are listed in Table 1. After curing, an average thickness of 6.43 ± 0.10 mm was reached.

Material	Type	Nominal ply thickness
CFRP-UD	MTM44-1/IMS65(24K)-268-32%RW	0.255 mm
CFRP-woven	MTM44-1/CF5804A-40%RW-DC	0.322 mm
GFRP-woven	MTM44-1/GF0903-40%RW	0.101 mm
Steel	X10CrNi18-8	0.125 mm
Elastomer	AA8DPZ	0.500 mm

Table 1: Sample constituents and their nominal thicknesses.

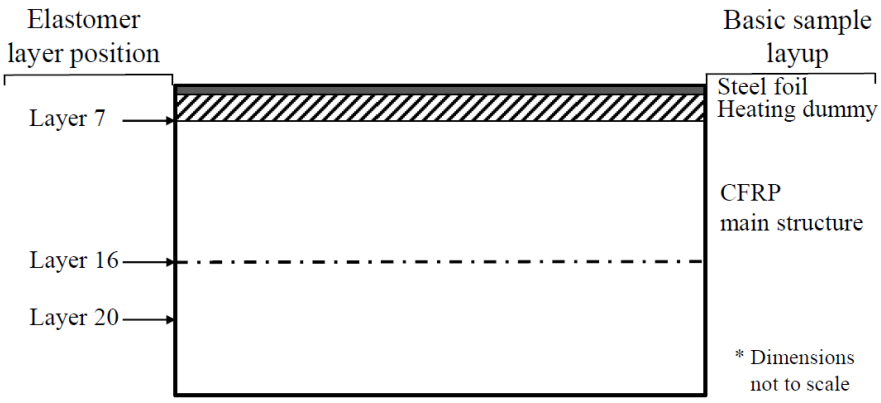

Figure 1: Schematic layup of impact specimens.

2.2 Experimental procedure

The low velocity impact tests were conducted with a CEAST Fractovis drop weight tower according to ASTM D7136 [14]. The 100 mm × 150 mm samples were fixed with four rubber clamps over a flat support with a 75 mm × 125 mm rectangular cut-out. It should be noted that the samples showed a slight curvature of approximately 1 mm over 150 mm side length because of the asymmetric layup. The difference in the thermal expansion coefficients of the constituents, especially of steel and CFRP, induce inner stresses in the hybrid material which cause the curvature. This curvature prevented an entirely flat support during impact. The samples were impacted once with a steel indentor with a hemispherical tip (20 mm diameter) containing a piezo-electric load cell. Six different energy levels between 5 and 50 J were tested. The energy was set by the combination of weight and drop height. The tested energy levels with the related test parameters are summarized in Table 2. Each configuration was tested three times at each energy level which results in 54 tested samples.

Desired energy level (J)	Mass (kg)	Measured velocity (m/s)
5	1.99	2.18 ± 0.01
9	1.99	2.98 ± 0.02
16	1.99	3.97 ± 0.02
28	5.99	3.04 ± 0.00
37	5.99	3.50 ± 0.00
50	5.99	4.06 ± 0.00

Table 2: Parameter combination for tested impact energy levels.

Following the impact tests, the samples were visually inspected on front and backside and the indentation depth was measured with a depth gauge. Afterwards, the delaminations were investigated by ultrasonic testing. This method can determine the exact position of every delaminated layer in pure composite specimens. However, the multi-material structure induces severe scattering of the ultrasonic waves which hinders the detection of delaminations in through-thickness direction. The same limitation was reported by Sarlin et al. for Scanning Acoustic Microscopy analysis [11]. Computer Tomography as well as the analysis of microsections also did not generate satisfactory results. As a consequence, merely the projected area of all delaminations were considered for evaluation.

3. RESULTS

Visual examination of the front side revealed hemispherical impact craters, which were barely visible up to and including 28 J impact energy. The samples having the elastomer layer in layer 7 showed bumps surrounding the impact crater at very high impact energies of about 50 J. On the back side fibers started to protrude out of the surface at 28 J. With increasing impact energy, a crack developed in longitudinal direction of the sample reaching a length of 20 mm at a 50 J impact. The position of the elastomer layer in the layup had no influence on the extend and geometry of front side or back side damage.

Figure 2(a) illustrates the effect of the elastomer layer position on the indentation depth. In the low energy regime (5 and 9 J) the elastomer layer position had almost no influence on the depth of the dent. At impact energies $\geq$ 16 J the indentation depth was the smallest for configuration L16, where the elastomer was positioned in the middle plane. Placing the elastomer in the lower third of the CFRP structure (L20), increased the depth by 0.04-0.06 mm or 11-63 %. When the elastomer was positioned in layer 7, the indentation depth was increased by 0.11-0.23 mm corresponding to a rise of 25-140 % in comparison to L16.

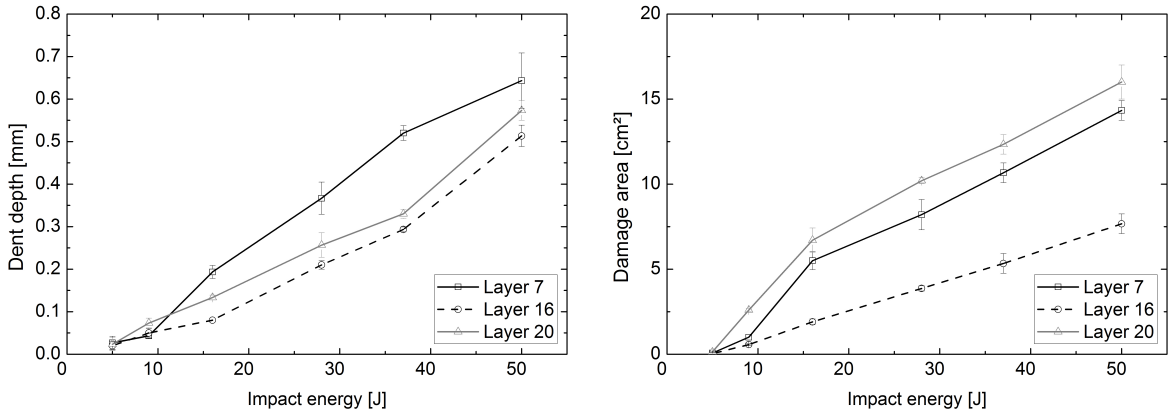

(a) (b)

Figure 2: Effect of the elastomer layer position on (a) the indentation depth and (b) the delamination area.

Delaminations started to develop at energies higher than 5 J, shown in Figure 2(b). The delaminated area increases linearly with the impact energy for configuration L16. The other configurations show a sharp increase of the damage area until 16 J and then also a linear progression with a slightly higher increase than L16. Consequently, the delaminations are 80-190 % larger for configuration L7 than for L16 and 100-370 % larger for configuration L20.

Figure 3 shows the influence of the elastomer layer position on the amount of the absorbed energy. When the impact energy was very low (5 J) approximately 23 % of the impact energy are absorbed from each sample configuration. With increasing impact energy the energy absorption rises. Initially, the amount of absorbed energy rises fast for the configurations L7 and L20, L16 lags behind the other configurations until 37 J. At 50 J impact energy L16 and L20 absorb approximately 4 % more energy than L7.

Figure 4(a) illustrates the maximum displacement of the indentor during impact versus the impact energy. The maximum deformation rises with increasing impact energy but without linear dependance, the values show practically no deviation. The deformation of L7 is the smallest at each impact energy. L20 deforms 0.2-0.3 mm more than L7, and L16 0.3-0.5 mm more than L7. In Figure 4(b) the impactor displacement evolutions are illustrated examplarily for a 28 J impact. Again, the diagram shows the highest maximum deformation for L16 and also the longest response time, whereas the response time of configuration L7 is the shortest.

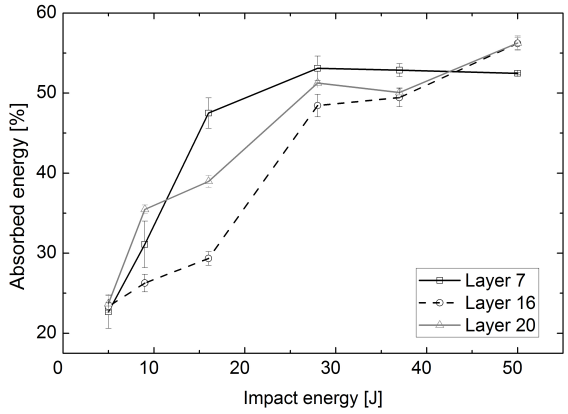

Figure 3: Effect of the elastomer layer position on absorbed energy.

4. DISCUSSION

In Figure 4 configuration L7 shows the smallest displacement and the shortest response time compared to the other configurations. This signifies the highest stiffness, which leads to a high energy absorption (Figure 3) resulting in a large destruction in case of impact (Figure 2). In comparison, configuration L16 shows the largest deformation and the longest response time, which shows a comparably low stiffness resulting in a lower energy absorption by damage. The reason is the positioning of the elastomer layer in the center of the CFRP structure and thus a partition into two single structures with bisected thickness. This leads to a minimization of the

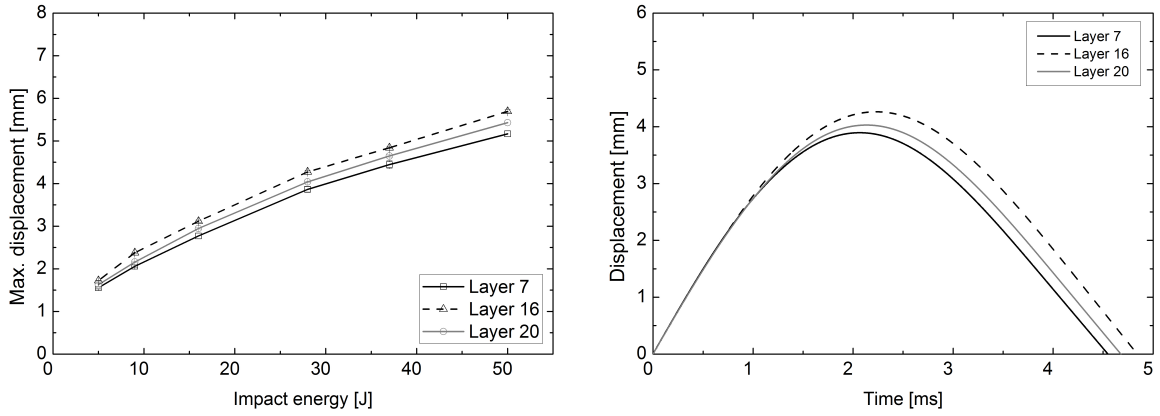

(a) (b)

Figure 4: (a) Effect of the elastomer layer position on the maximum displacement and (b) impactor displacement curves for all three sample configurations at 28 J impact energy.

delaminated area (Figure 2(b)) and the dent depth (Figure 2(a)). In contrast, the structure of L7 is practically not interrupted because the elastomer is placed directly beneath the comparably smooth heating structure and does not influence the stiffness of the actual CFRP support structure. The CFRP structure of configuration L20 is eccentrically interrupted by the elastomer in the lower third of the structure. Consequently, its stiffness is situated between configuration L7 and L16.

Considering only the stiffness of the structure, the overall destruction of L7 should be the highest. However, Figure 2(b) shows a larger damage area for configuration L20 than for L7. The reason could be observed in other tests before [12]: When the elastomer is located in a position very close to the steel surface, the surface damage is the predominant damage type. The smoothness and elasticity of the elastomer leads to a large elastic deformation of the upper layers during impact. The steel follows this deformation and while the yield point is exceeded, the steel is deformed plastically. This plastic deformation dissipates a larger amount of the impact energy protecting the underlying CFRP structure partially. As a result, the damage area of configuration L7 is smaller than that of the less stiff configuration L20.

A further consideration is that the insertion of the elastomer layer not only decreases the stiffness but also interrupts the propagation of so-called pine tree crack pattern. Those cracks start as matrix cracks directly on the impacted surface. The damage propagates from the surface into deeper layers through the formation of intra-ply cracks and delamination [15]. Those cracks naturally propagate in the depth and the width of the structure and the deeper the layer the wider the delaminations. The elasticity of the elastomer prevents the damage propagation into deeper layers and thus also in the width of the structure, which reduces the damage area especially in configuration L16. Since an elevation resolution of the delaminations is not possible by standard ultrasonic C-scans, this effect has to be verified by other examination methods as CT-scan or microsections.

From a perspective of severity of damage, the positioning of the elastomer layer in the central plane of the CFRP structure is favoured. However, the application in aerospace structure generally requires a high stiffness- and strength-to-weight ratio. The actual reduction of the bending stiffness through the variation of the elastomer layer position in case of impact has to be determined in further tests, for example compression after impact tests.

5. CONCLUSIONS

The impact behaviour of a CFRP/GFRP/steel/elastomer hybrid-material structure has been investigated in the presented study. In order to investigate the influence of the position of the elastomer layer, samples with three different elastomer layer positions were subjected to low-velocity impacts at different energy levels. The following conclusions can be drawn from the results of the study:

- The position of the elastomer influences the bending stiffness of the structure through a quasi-division into two single structures with two bending stiffnesses depending on their respective thickness. The thicker part rules the overall bending stiffness of the structure and therefore the severity of the damage.
- Consequently, a minimization of indentation and delamination is reached by locating the elastomer in the middle plane of the CFRP structure. The overall bending stiffness is minimized by the division of the CFRP structure into to equal parts.
- The positioning of the elastomer layer in the upper layers of the structure causes a comparatively large destruction of the surface by indentation but reduces the damage area. The reason is a plastic deformation of the overlying steel foil, which permanently displaces the soft and elastic elastomer.

The applicability in aeronautics and space has to be verified regarding the demanded strength and stiffness values by further tests such as compression after impact tests. The examination of the crack pattern will provide information regarding the influence of the elastomer layer on the crack propagation.

References

[1] G. B. Chai and P. Manikandan. Low velocity impact response of fibre-metal laminates - a review. *Composite Structures*, 107:363–381, Jan 2014.

[2] N. Tsartsaris, M. Meo, F. Dolce, U. Polimeno, M. Guida, and F. Marulo. Low-velocity impact behavior of fiber metal laminates. *Journal of Composite Materials*, 45(7):803–814, 2011.

[3] D. Stefaniak, E. Kappel, B. Kolesnikov, and C. Hühne. Improving the mechanical performance of unidirectional CFRP by metal-hybridization. In *Proc. ECCM15 - 15th European Conference on Composite Materials*, 2012.

[4] G.H. Jilbert and J.E. Field. Synergistic effects of rain and sand erosion. *Wear*, 243(1-2):6–17, 2000.

[5] A.A. Fyall. Practical aspects of rain erosion of aircraft and missiles. *Philosophical Transactions of the Royal Society A: Mathematical, Physical and Engineering Sciences*, 260(1110):161–167, 1966.

[6] O. Gohardani. Impact of erosion testing aspects on current and future flight conditions. *Progress in Aerospace Sciences*, 47(4):280–303, 2011.

[7] N. Miyazaki. Solid particle erosion behavior of frps with prior impact damage. *Journal of Composite Materials*, 41(6):703–712, 2006.

[8] W.J. Cantwell and J. Morton. The impact resistance of composite materials - a review. *Composites*, 22(5):347–362, 1991.

[9] M.O.W. Richardson and M.J. Wisheart. Review of low-velocity impact properties of composite materials. *Composites Part A: Applied Science and Manufacturing*, 27(12):1123–1131, 1996.

[10] K.V. Pool, C.K.H. Dharan, and I. Finnie. Erosive wear of composite materials. *Wear*, 107(1):1–12, 1986.

[11] E. Sarlin, M. Apostol, M. Lindroos, V.-T. Kuokkala, J. Vuorinen, T. Lepistö, and M. Vippola. Impact properties of novel corrosion resistant hybrid structures. *Composite Structures*, 108:886–893, 2014.

[12] D. Niewerth, D. Stefaniak, and C. Hühne. The response of hybrid composite structures to low-velocity impact. In *ICEM 16 - 16th International Conference on Experimental Mechanics*, 2014.

[13] Umeco. MTM44-1 – PDS1189_07.12_Issue8, 2012.

[14] ASTM D 7136/D 7136M-12. Standard test method for measuring the damage resistance of a fiber-reinforced polymer matrix composite to a drop-weight impact event. Standard, ASTM International, West Conshohocken (PA, USA), 2012.

[15] Serge Abrate. Impact on composite structures. 1998.